Structure functions from HERA

David Reyna[a]*

[a]DESY - FH1, Notkestraße 85, 22607 Hamburg, Germany.

Recent results from structure function analysis at HERA are reviewed. Particular emphasis is placed on the extreme kinematic regions which allow measurements of the structure functions F_L and xF_3. In addition, the latest $F_2^{c\bar{c}}$ results and an investigation of the transition region at very low Q^2 are presented.

1. Introduction

At HERA, results on the proton structure function F_2 have emerged as one of the true flagships of high-precision experimental data. The original fixed target results from SLAC[1], which first showed the existence of Bjorken scaling, have been extended over five orders of magnitude in the four-momentum transfer squared Q^2 and four orders of magnitude in the Bjorken scaling variable x.

The high precision and large kinematic coverage from HERA have allowed high quality tests of QCD derived evolution. Using fits to the data at low values of Q^2 to fix the parton distribution functions, results from the DGLAP evolution equations [3] are in very good agreement with the data over the whole kinematic range. In addition, the reach into lower values of x has seen strong evidence of scaling violations due to the increasing gluon content.

More complete analysis of the primary F_2 measurement and its implications can be found elsewhere [2]. Rather, this paper will focus on the extreme kinematic regions which are available for analysis with this high-statistics data set.

2. Kinematics and Structure Functions

The kinematics of lepton-proton Deep Inelastic Scattering (DIS), $e(k) + p(P) \to e(k') + X$, is defined by the Lorentz scalars Q^2 and Bjorken x which, in the absence of QED radiation, can be expressed as

$$Q^2 = -q^2 = -(k-k')^2, \quad (1)$$

$$x = \frac{Q^2}{2P \cdot q} \; (0 \leq x \leq 1), \quad (2)$$

where k and P are the four-momenta of the incoming particles and k' is the four-momentum of the scattered lepton. The fractional energy transferred to the proton in its rest frame,

$$y = \frac{p \cdot q}{p \cdot k} \; (0 \leq y \leq 1), \quad (3)$$

is related to Q^2 and x via $Q^2 = xys$, where $s = (k+p)^2 \simeq 4E_e E_P$ is the square of the total center-of-mass energy of the lepton-proton collision.

The double differential cross section for inclusive eP scattering can be written as

$$\frac{d^2\sigma}{dx\,dQ^2} = \frac{2\pi\alpha^2}{xQ^4}\left[Y_+ F_2(x,Q^2) - y^2 F_L(x,Q^2) - Y_- xF_3(x,Q^2)\right], \quad (4)$$

where $Y_\pm = 1 \pm (1-y)^2$ and x and Q^2 are defined at the hadronic vertex. F_2 is the familiar structure function containing mostly parton distribution information, F_L is the longitudinal structure function and F_3 contains the effects of γZ° interference and parity violation. By positivity constraints, F_L must obey the relation $0 \leq F_L \leq F_2$. The kinematic factors restrict the contribution of F_L to the cross section to the region of high y while the xF_3 term will only contribute in the kinematic range of both high y and high x.

Most experimental results are quoted in the so-called reduced cross section, defined as

$$\sigma_r \equiv \frac{Q^4 x}{2\pi\alpha^2 Y_+}\frac{d^2\sigma}{dx\,dQ^2} = F_2 - \frac{y^2}{Y_+}F_L - \frac{Y_-}{Y_+}xF_3. (5)$$

If one excludes the extreme kinematic regions of high x and high y, then this reduces to the normal

*On behalf of the H1 and ZEUS Collaborations.

relationship that $\sigma_r \simeq F_2$. However, with the increased statistics and increased kinematic coverage that are now available to HERA, it is exactly these extreme regions that are causing interest.

3. Measurement of xF_3

In the past, this structure function has only been accessible by neutrino experiments. However, access to F_3 is available at HERA since the contribution to the cross section in lepton proton scattering changes sign with the charge of the incoming lepton.Therefore, by comparing the recent 1998 data, taken with electrons, with the previous 1997 data set, using positrons, the direct effects of the xF_3 term can be seen (Fig. 1) in the high x, high y kinematic domain, as expected.

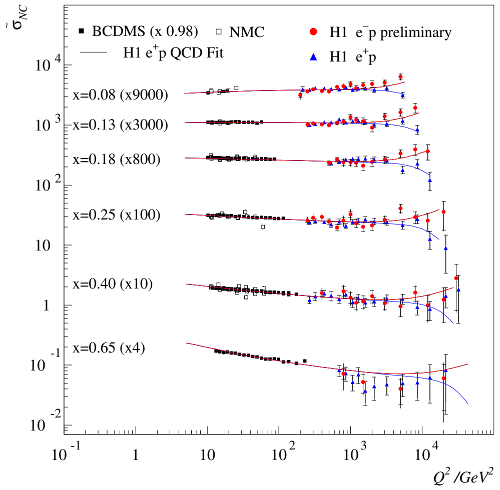

Figure 1. The reduced cross section in the 6 highest available x bins as a function of Q^2. The filled circles show the 1998 data using electrons while the filled triangles show the previously published positron data. With increasing values of Q^2, which correspond to increasing y, the deviation between the electron and positron data sets, attributable to the xF_3 contribution, can be seen.

By taking the difference of the two data sets, with the appropriate kinematic factors to account for the different proton beam energies from the different years (820 GeV in 1997; 920 GeV in 1998), the ZEUS collaboration has recently released results on an extraction of xF_3 (Fig. 2). The current errors are dominated by the limited luminosity of the electron sample, which is less than half that of the positron data set. The data are currently consistent with QCD calculations and the expectation for increased electron luminosity in the future should allow better precision.

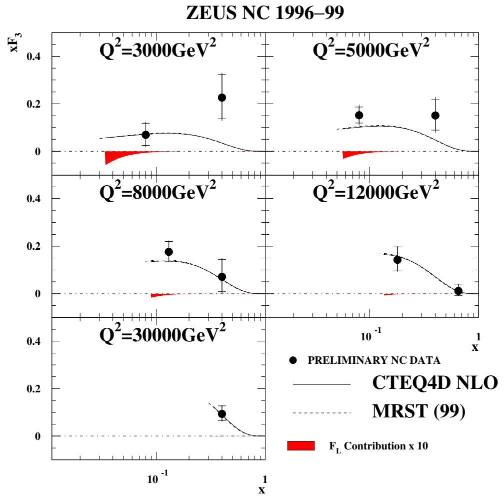

Figure 2. Preliminary extraction of xF_3 from the ZEUS collaboration using electron data from 1998 and positron data from 1999 and 1994-1997. QCD calculations with 2 different parton distributions functions are shown to be in good agreement with the data. In addition, the expected contribution of F_L, magnified by an order of magnitude, is also shown in the shaded area.

4. Extraction of F_L

The H1 collaboration has previously extracted F_L by extrapolating a fit to the data at intermediate and low values of Q^2 and intermediate x, where the statistics are high and the relation $\sigma_r \sim F_2$ holds, down to low x (which at fixed Q^2 corresponds to high y). Deviations from this fit are seen and are attributed to F_L [5].

In addition, H1 has recently pursued a systematically independent method by the measurement of the reduced cross-section derivative:

$$\frac{\partial \sigma_r}{\partial \ln y} \equiv -\frac{\partial F_2}{\partial \ln y} - F_L \cdot 2y^2 \cdot \frac{2-y}{Y_+^2} + \frac{\partial F_L}{\partial \ln y} \cdot \frac{y^2}{Y_+}. \quad (6)$$

This method relies on the assumption that the derivative $\partial\sigma_r/\partial \ln y$ is a linear function of $\ln y$ up to large y. For the measurement of $\partial\sigma_r/\partial \ln y$, the data are binned in y and the differences $\Delta\sigma_r$ are calculated between cross-section points adjacent in y. The function $\partial F_2/\partial \ln y = A \ln y + B$ is fit to the data for $y < 0.2$. In Figure 3, such a straight line fit can be seen to describe the data very well for low y. In addition, the F_2 values thus determined are found to be in good agreement with the results of the QCD fit. Also shown in Fig. 3 are comparisons with NLO QCD calculation using different assumptions on F_L. The extrapolation of the straight line to high y represents the contribution of F_2 and the deviations at high y were attributed to the contribution from F_L. An important feature of this method is a

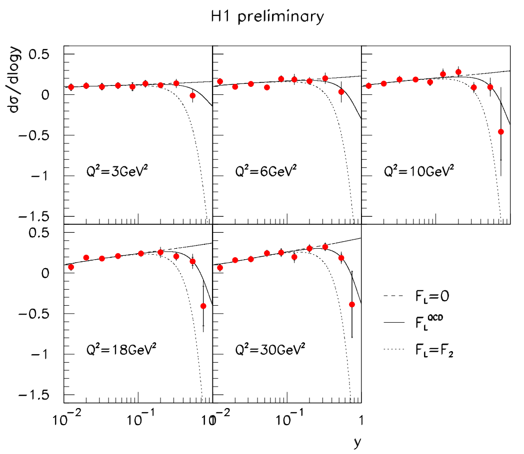

Figure 3. Measurement of the derivative $\partial\sigma_r/\partial \ln y$ for different Q^2 bins. The curves represent the results of the standard QCD fit (solid curve) and the results for the extreme assumptions $F_L = 0$ (dashed curve) and $F_L = F_2$ (dotted curve).

partial cancellation of systematic errors. In addition, it should be noted that the contribution from $\partial F_L/\partial \ln y$ to the derivative in Eq. 6 is corrected by assuming NLO QCD behavior.

The F_L results from the derivative method are shown in Fig. 4 (stars) together with the results from the previously reported subtraction method[5] (closed points). While both methods use the same data, it is reassuring to see that all F_L values are consistent since the uncertainties in the measurements are, by construction, different. In addition, the derivative method permits access

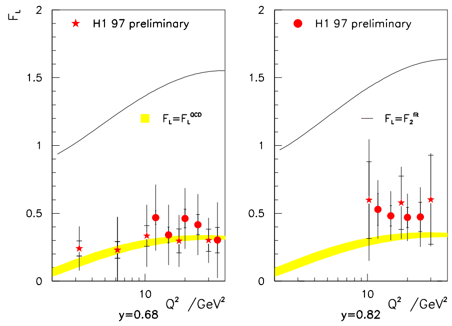

Figure 4. Determination of F_L using the subtraction method [5] (closed points) and the derivative method (stars), which extends to lower Q^2. The two determinations used the same data set. The narrow band represents the uncertainty range in F_L as calculated with the gluon and quark distributions determined from a NLO QCD fit to F_2.

to lower Q^2 (down to 3 GeV^2) than the previous measurement since, at low Q^2, the extrapolation based on QCD is uncertain. The determined F_L is compatible with QCD predictions, shown as bands in Fig. 4, based on the gluon and quark distributions determined from the NLO QCD fit to the F_2 data, although it seems to be systematically above the QCD prediction at highest y.

5. Measurements of F_2 at very low Q^2

The unqualified success of the QCD evolution in describing the experimental data from Q^2 of a few GeV and up has also driven the investigation of the critical transition region at low Q^2. Early results of data from runs in which the interaction vertex was shifted by 60cm in the electron direction (*shifted vertex data*[4]) showed surprising agreement with the results from pQCD predictions even down to $Q^2 \sim 1$ GeV. However, total cross sections in the photoproduction region ($Q^2 \sim 0$) are normally compared with Regge inspired models with relative success. Recent interest has therefore focused on the transition between the low Q^2 hadronic regime and the intermediate and high Q^2 partonic regime.

The ZEUS collaboration has recently installed a new detector system (BPT [6]) for measuring scattered electrons at very low scattering angles and thus very low Q^2 ($0.04 < Q^2 < 0.8$). It can be seen in Figure 5 that the data[7] from the ZEUS BPT, being quite consistent with the

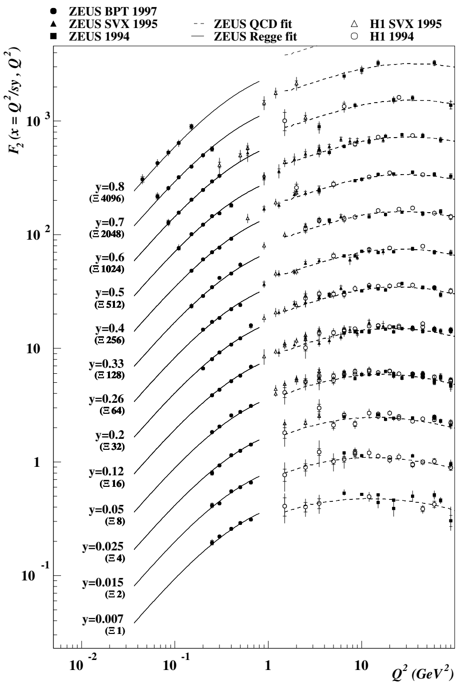

Figure 5. The reduced cross section in fixed y bins as a function of Q^2. All published data from H1 and ZEUS are shown including the shifted vertex data from 1995[4] in the region of Q^2 between 1 and 5 GeV. Also shown are the new ZEUS BPT results[7] (closed circles) at $Q^2 < 1$GeV. The solid line represents a Regge based fit to the low Q^2 data while the dashed line represents an extension of the pQCD based fit from higher Q^2 down to 1.5GeV^2.

Regge based models, are still largely dominated by the hadronic degrees of freedom. However, by noticing the lack of agreement between the extrapolations of the Regge based model and the pQCD based fits, one can see that more study is clearly necessary in the area of $Q^2 \sim 1$ GeV to better understand this transition.

6. Measurement of $F_2^{c\bar{c}}$

The scaling violations in F_2 at low x have been attributed to a rising gluon population. To confirm the universality of this gluon distribution, an analogous structure function, $F_2^{c\bar{c}}$, in which evidence of charm quark production is seen in the final state, has been investigated. Due to the high mass, charm quark production in DIS is expected to be dominated by the boson-gluon fusion process. The likelihood of such a process is directly dependent on the gluon distribution in the proton.

The boson-gluon fusion process can be convoluted in perturbative QCD with the measured gluon distribution, extracted from the inclusive F_2 measurements, to produce a prediction for $F_2^{c\bar{c}}$. Experimentally, events with a clear D^* signal in the final state are corrected for branching ratios and detector and acceptance limitations to create the analog of the inclusive reduced cross section.

The ZEUS collaboration has recently published results [8] on $F_2^{c\bar{c}}$ which improve on the previous measurements [9]. As well as increased statistics, the recent results include an analysis of the $D^* \to K3\pi\ \pi_s$ decay mode in addition to the previously analyzed $D^* \to K\pi\ \pi_s$ decay mode, where π_s is the slow pion emitted in the decay $D^* \to D\pi$.

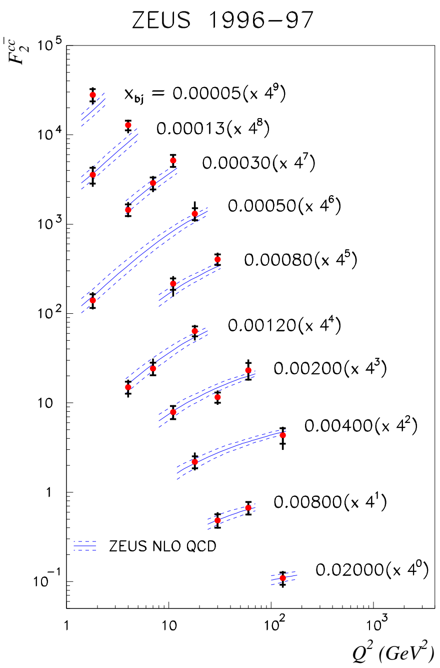

Figure 6. Data from ZEUS on $F_2{}^{c\bar{c}}$ versus Q^2. Strong scaling violations are clearly visible. The shaded region corresponds to the results of QCD calculations using the gluon distribution of the proton as extracted from inclusive F_2 measurements.

In Fig. 6 one can see that the scaling violations are quite evident, demonstrating the expected gluon dominance. In addition, the ratio of $F_2^{c\bar{c}}$ to F_2 has been investigated and seen to fall with falling Q^2 from about 30% at $Q^2 \sim 60$ to 10% at $Q^2 \sim 2$. This implies that the gluonic component of the sea falls with falling Q^2. These results are well described by the QCD calculations.

7. Summary

The structure function measurements from HERA provide many more interesting tests of QCD that could not be included in this paper. For a more complete coverage of the current state of this subject one should also refer to other articles [2],[10] and to the the workshop on Deep Inelastic Scattering and QCD held at Liverpool in April, 2000 [11]. I have concentrated here on the extreme kinematic regions available at HERA which have been explored to measure the additional structure function xF_3 and extract a value for F_L. Also, $F_2^{c\bar{c}}$ has been presented as a test of the gluon distribution of the proton. In addition, the very low Q^2 transition between the partonic (pQCD) and the hadronic (Regge) regimes has been explored. All these results are currently in agreement with the QCD predictions.

REFERENCES

1. E.D. Bloom et al., Phys. Rev. Lett. 23, 930 (1969); M. Breidenback et al., Phys. Rev. Lett. 23, 935 (1969).
2. Max Klein, Proceedings of the 19th International Symposium on Lepton and Photon Interactions at High-Energies (1999).
3. G. Parisi, Proc 11th Recontre de Morionde (1976); G. Altarelli & G. Parisi, Nucl. Phys. B126 (1977) 298;
   V. Gribov & L. Lipatov, Sov. Jour. Nucl. Phys. 15 (1972) 438; L. Lipatov, Sov. Jour. Nucl. Phys. 20 (1975) 94; Y. Dokshitzer, Sov. Phys. JETP 46 (1977) 641.
4. H1 collaboration, I. Abt et al., Nucl. Phys. B497 (1997) 3; ZEUS Collaboration, J. Breitweg et al., Eur. Phys. J. C7 (1999) 609.
5. H1 Collab., C. Adloff et al., Phys. Lett. 393B (1997) 452.
6. Qiang Zhu, Proceedings of the VII International Conference of Calorimetry in High Energy Physics (1997).
7. ZEUS Collaboration, J. Breitweg et al., Phys. Lett. B487 (2000) 1-2, 53-73
8. ZEUS Collaboration, J. Breitweg et al., Eur. Phys. J. C12 (2000) 1.
9. H1 Collaboration, C. Adloff et al., Z. Phys. C72 (1996) 593; ZEUS Collaboration, J. Breitweg et al., Phys. Lett. B407 (1997) 402.
10. G. Altarelli, R. Ball and S. Forte, CERN-Th/2000-010, hep-ph/00001157.
11. Proc. of the 8th International Workshop on Deep Inelastic Scattering and QCD, to be published in Nucl. Phys. B (Proc. Suppl.)